THE MEASURED RESPONSE OF ULTRA-THIN AND THIN WHITETOPPING TO ENVIRONMENTAL LOADS

Julie M. Vandenbossche
Minnesota Department of Transportation
1400 Gervais Ave. MS 645
Maplewood, MN 55109

ABSTRACT

The technique of whitetopping asphalt concrete pavements with a thin (102-mm to 152-mm thick) or ultra-thin (51-mm to 102-mm thick) concrete overlay is becoming more common. The increase in use of thin whitetopping (TW) and ultra-thin whitetopping (UTW) has amplified the need for a comprehensive design procedure. The purpose of this research project is to develop a better understanding of the behavior of thin and ultra-thin whitetopping by measuring the responses of the pavements to various environmental loadings.

A 345-mm asphalt concrete pavement on I-94, at the Minnesota Road Research (Mn/ROAD) facility, was whitetopped with a fiber-reinforced concrete overlay in October 1997. The experimental design features six test cells with various thicknesses, joint patterns and types of fibers. Each cell is instrumented with dynamic and static strain, temperature and moisture sensors. Temperature, moisture and static strain data have been collected continuously since construction.

Strain gages were used to measure the effects of moisture and temperature changes in the pavement. An evaluation of the data over time indicates seasonal changes occur in the quality of bond between layers, which has implications for changes in load-related stress over time. Both thermal and moisture changes in the overlay have a significant effect on the shape of the slab. Strain measurements revealed the complexity of the relationship between changes in temperature and/or moisture and slab deformation. This relationship must be clearly defined before an analysis of the response of the overlay to an applied load can begin. This study helped characterizing these relationships.

Subject Area: thin whitetopping, ultra-thin whitetopping, thermal strain, drying shrinkage

INTRODUCTION

The technique of whitetopping asphalt concrete pavements with a thin (102-mm to 152-mm thick) or ultra-thin (51-mm to 102-mm thick) concrete overlay is becoming more common. The two primary factors necessary for long-term performance from a thin overlay are maintaining a good bond between the overlay and the asphalt so load-related stresses can be reduced and using short joint spacings to reduce curling and warping stresses and bending stresses produced by applied loads. The increase in use of thin whitetopping (TW) and ultra-thin whitetopping (UTW) has amplified the need for a comprehensive design procedure. Efforts in this direction have already been initiated.(2, 3) An in-depth analysis is needed to better characterize the response of a TW and an UTW to both applied and environmental loads so that they can be implemented into a more comprehensive design procedure. This paper quantifies the effect of environmental considerations that must be accounted for when predicting the performance life of TW and UTW.

Instrumented TW and UTW test sections were constructed so that the response of the overlay to applied and environmental loads could be measured and then correlated to performance for a range of design parameters. The test sections were constructed on I-94, at the Minnesota Road Research (Mn/ROAD) facility. A 345-mm asphalt concrete pavement was whitetopped with a fiber-reinforced concrete overlay in October 1997. Each test section was milled to the depth of the concrete overlay so that the existing surface elevation would be maintained. The experimental design features six test cells with various thicknesses, joint patterns and types of fibers. The test cells are instrumented with dynamic and static strain, temperature and moisture sensors. Two weather stations are also located at each end of the test facility so detailed climatic data is available at 15 minute intervals 365 days of the year. Test sections considered in this study include a 76-mm overlay with 1.5 m x 1.8-m panels, a 102-mm overlay with 1.2 x 1.2-m panels, and a 152-mm overlay with 3.0 m x 3.7-m panels.

TEMPERATURE CHARACTERIZATION

The average annual high temperature at Mn/ROAD since the TW and UTW test sections were constructed is 33 °C with an average annual low of –29 °C. Large temperature ranges, such as this, can contribute to high thermal strains caused by uniform expansion and contraction. Large daily temperature fluctuations can produce large temperature gradients in the slab resulting in high curling stresses. The first step in analyzing the effects of environmental load is to determine the range of temperatures and the magnitude of the linear temperature gradients found in TW and UTW. It is evident by the range of ambient temperatures that the temperature of the overlay will vary greatly throughout the year. The magnitude of the temperature gradients that develop and the frequency at which they are present is not as apparent. Each TW and UTW test section was instrumented with thermocouples at various depths in the concrete and asphalt. Thermocouples were placed at the midpanel and at midslab, adjacent to the lane/shoulder joint. The top thermocouple is located 13 mm below the pavement surface. A thermocouple was also embedded into the bottom of the overlay at the concrete/asphalt interface. Temperature data from the thermocouples has been collected continuously from the time of construction at 15-minute intervals.

Thermocouple data was used to quantify the magnitude and frequency of the temperature gradients that developed in the 76-, 102-, 152-mm overlays throughout a 1-year period. Cumulative frequency distribution graphs were developed for linear temperature gradients calculated every 15 minutes throughout the year for each test section. A positive gradient occurs when the top of the slab is warmer than the bottom of the slab and a negative gradient occurs when the top of the slab is colder. The cumulative frequency graphs for the midpanel thermocouple data collected in each test section are provided in figure 1. Table 1 contains the maximum monthly positive and negative gradients at each location. A summary of the average values for both locations within each test section is presented below.

<u>76-mm Overlay</u>

1.) The gradient is between –0.40 °C/cm and 0.80 °C/cm 95 percent of the time
2.) Maximum positive gradient is 1.23 °C/cm
3.) Maximum negative gradient is –0.82 °C/cm
4.) The mean gradient is –0.20 °C/cm
5.) A positive gradient is present 32 percent of the time while a negative gradient is present 63 percent of the time

102-mm Overlay

1.) The gradient is between –0.35°C/cm and 0.60 °C/cm 95 percent of the time
2.) Maximum positive gradient is 0.81 °C/cm
3.) Maximum negative gradient is –0.61 °C/cm
4.) The mean gradient is –0.20 °C/cm
5.) A positive gradient is present 36 percent of the time while a negative gradient is present 57 percent of the time

152-mm Overlay

1.) The gradient is between –0.25 °C/cm and 0.45 °C/cm 95 percent of the time
2.) Maximum positive gradient is 0.96 °C/cm
3.) Maximum negative gradient is –0.63 °C/cm
4.) The mean gradient is –0.15 °C/cm
5.) A positive gradient is present 39 percent of the time while a negative gradient is present 51 percent of the time

The graphs in figure 1 show the gradients have a skewed normal distribution with a higher frequency of negative gradients but a lager maximum positive gradient. Table 1 shows the temperature differentials between the top and bottom of the slab are larger for the 152-mm overlay. However, the average magnitude of the gradients is similar for all of the overlays because smaller temperature differentials produce large gradients when the overlay thickness is reduced to 76 and 102 mm. This illustrates the need to look at temperature gradients and not just temperature differentials. The three temperature differentials considered in the development of the current design procedure include +8.3, +2.7, and –5.5 °C for overlays 50, 102, and 152-mm thick.(3)

The time of year that large gradients develop is shown in Table 1. Large negative temperature gradients mainly occur in the winter when extremely low air temperatures are common. Large negative gradients also occur during the daytime in the summer months when the high ambient temperatures heat the pavement and then the pavement surface is rapidly cooled by an afternoon shower. The curling stresses that develop as a result of the negative gradients in the winter are significantly different than the stresses that develop in the summer. For example, if curling were measured on a summer afternoon when pavement temperatures are high the joints will most likely be locked, which will reduce the amount of curling that will develop. However, if the pavement temperature is lower, such as on a spring night, the joints will open allowing the edges and corners of the slab to curl upward more freely. Increasing the thickness of the overlay makes the overlay less susceptible to large negative gradients as a result of a summer afternoon shower because smaller changes in temperature differentials have less of an impact on the gradients in thicker slabs.

Large positive gradients develop more frequently in the spring and summer. In the spring, the lower layers of the pavement are still cool from the winter, creating large positive gradients when the warm spring air heats up the pavement surface. The intense summer heat also produces large gradients in the summer. As with the negative gradients, the higher pavement temperature in the summer will lock the joints and reduce the curling potential more than in the spring when the pavement temperature is lower.

THERMAL STRAINS

The next step is to determine the response of the overlay to thermal loads based on the frequency and magnitude of the gradients that have been defined. The instrumented test sections contain static strain gages at 25 mm below the top of the concrete surface and 25 mm above the asphalt at midpanel, adjacent to the transverse joint, and adjacent to the longitudinal lane/shoulder joint. The gages located at midpanel and adjacent to the longitudinal lane/shoulder joint measure strains in the longitudinal direction and the gage adjacent to the transverse joint measure strains in the transverse direction. Strains resulting from a change in temperature were measured at the top and the bottom of the slab. The temperature and strain measured at the first zero gradient period of the day were used as the base value. The strains were plotted against daily changes in temperature at various times of the year for each test section.

Relationship between Strain and Change in Temperature

Strain has been plotted against change in temperature for a representative day in May in figures 2 through 9 for the 152-mm overlay and 76-mm overlays. Strain data was not provided for the 102-mm overlay for the sake of brevity since the response of the 76-mm and 102-mm overlays were quite similar. Each data series represents a 24-hour period of strain measurements resulting from a change in temperature. The maximum weighted average temperature of the overlay during the day was approximately 37°C with the minimum 15°C.

The first observation made was that the strain generated as the slab expanded was not equal to the strain generated as the slab contracted for an equivalent change in temperature. A loop is formed during daily temperature cycles with the top portion of the loop representing the strain path during expansion and the bottom portion the strain path during contraction. This results in a higher rate of strain during expansion than during contraction. As a result, an increase in strain of up to 50 microstrains can occur when the concrete is expanding compared to contracting for the same change in temperature. This phenomenon is more prevalent at the top of the slab and for thicker sections with longer panel lengths.

Strain gages can also be used to determine the temperature at which the joints lock-up preventing the slab from continuing to expand as the temperature increases. Strains measured parallel and adjacent to the longitudinal joint and at midpanel converge at the same level of strain indicating joint lock-up. The joint locks at the bottom of the slab at a lower temperature than at the top of the slab because the increased drying shrinkage that occurs at the surface creates a larger crack opening at the joint in the upper portion of the slab. The 3-mm joints sawed to a depth of 50 mm also create additional room for expansion at the surface. The top portion of the slab locks at approximately 25°C while the bottom portion locks around 20°C. There is a 75 microstrain and a 50 microstrain difference between the strain at which the top portion of the slab locks and the bottom portion locks for the 3.0-m panels in the 152-mm overlay and the 1.5-m panels in the 76-mm overlay, respectively.

Strains measured along the transverse joint did not converge to a maximum strain level because the asphalt shoulder is not capable of providing sufficient resistance to restrain the thermal expansion of the concrete overlay. The stiffness of the asphalt shoulder was low since the temperatures in the asphalt shoulder exceeded 35°C. The expansion that occurs in the transverse direction, which has less restraint, gives an indication of the magnitude of the stresses generated when the locked joints prevent the slab from expanding in the longitudinal direction. There was a difference in maximum strain of 150 microstrain for the top sensor and 200 microstrain at the bottom sensor between the locked joints and the transverse joint. The elastic

modulus of the concrete is 33,100 MPa so the stress generated as locked joints restrict the slab from expanding is approximately 6.6 MPa at the bottom of the slab and 5.0 MPa at the top of the slab. This shows the large restraint stresses that can be generated even in short (1.5 m) panels. Strains measured in the corner of the slab at a 45 degree angle to the lane shoulder joint exhibited a combination of the behavior seen in the longitudinal and the transverse direction. The strains did not completely converge as the temperature increased but they did taper slightly.

Seasonal Temperature Effects

Strains resulting from a change in temperature were also measured at the top and the bottom of the slab along the transverse joint for a day in December so comparisons could be made between the responses of the overlays at warm temperatures with those at colder temperatures. See figures 10 and 11. The maximum temperature in the overlay was approximately 9°C with a minimum temperature of 0°C. The strains measured during this time period for the 76-mm overlay did not converge to a maximum strain level, indicating the lane/shoulder joint did not lock-up. Figure 11 indicates the lane/shoulder joint did lock in the 152-mm overlay showing the asphalt shoulder is stiff enough to restrain concrete expansion if the temperature of the asphalt is sufficiently low. The lane/shoulder joints locked in the 152-mm overlay but not the 76-mm overlay because the panel width is twice as long in the 152-m overlay (5.7 m vs. 1.8 m). There was also a larger change in temperature over the 24-hour period (10°C vs. 8°C) in the summer. The magnitude of the strains was significantly smaller in December for both overlays because smaller temperature changes occurred throughout the day.

The strains produced by a given change in temperature in May are larger than the strains produced for the same change in temperature in December indicating that, along with an increase in the asphalt stiffness, there was an increase in the strength of the bond between the concrete and asphalt. These findings stress the importance of considering not only the temperature differential but also the average temperature throughout the depth of the pavement. Strain graphs from December also better reveal the nonuniform restraint between the asphalt and concrete. Equivalent increases in strain are not gained with each unit increase in temperature change. Instead stresses build up until the restraining stresses are exceeded and the concrete is allowed to expand or contract.

Slope Analysis

Obtaining bond between the two layers is essential for the long-term performance of thin and ultra-thin whitetopping. Bonding the two layers increases curling/warping stresses, which is partly offset by using a smaller joint spacing, but significantly decreases the stresses from the combined effect of curling and an applied load. Principles of superposition can be used to quantify the combined effects of curling and an applied load once it has been determined that the two layers are bonded. This assumption significantly underestimates the stresses if the overlay is unbonded. For this reason, it is extremely important to accurately characterize the bond between the two layers. Static strain gages were used to help determine if the overlay was bonded to the asphalt and to quantify the magnitude of strain that develops when a temperature gradient is present.

The rate at which strain increases with changing temperature is higher at the bottom of the slab than the top of the slab. This relationship is observed by comparing the increase in slope in the strain versus temperature measurements made at the bottom of the slab to measurements taken at the top of the slab. During the morning hours as the sun rises and heats up the surface of

the overlay, it creates a higher temperature on the top of the overlay than the bottom of the overlay. The bottom portion of the slab, which is bonded to the asphalt, restricts thermal expansion in the upper portion of the slab thereby reducing the slope. The bottom of the overlay begins to expand as the temperature increases at the bottom of the overlay and in the asphalt layer. The thermal coefficient of asphalt is 3.5 times greater than that of concrete so the bottom of the overlay expands at a faster rate than if the concrete was not bonded to the asphalt layer. The difference in the slope of the strains measured at the bottom and the top of the slab increases with increasing slab thickness because it takes a longer period of time for the temperature at the bottom of the slab to equal that at the top of the slab since the points at which the strains are measured are further apart. It may not be intuitive that a viscoelastic material, such as asphalt, can effect the rate of expansion of a "rigid" concrete material but evidence of this is also seen when transverse cracks in the asphalt reflect upward into the overlay during the winter. The higher slope for the strain data at the bottom sensor when compared to the top sensor also indicates that the overlay is not curling when temperature gradients are present.

Changes in bond strength that occur throughout the year with changing temperatures in the asphalt are another important consideration in predicting the performance of the overlay. A comparison was made between the strain data collected at various times of the year to quantify the seasonal effects of the bond strength. Strains measured in May, October and December were plotted against change in temperature and compared. See figures 2 through 13. Slightly higher slopes were observed at the bottom of the slab than the top of the slab during all three months, indicating that the overlay and the asphalt were at least partially bonded. The difference between the slopes of the strains at the top and the bottom of the slab increased as the temperature of the asphalt decreased and the stiffness and bond strength of the asphalt increased. This trend stresses the importance of considering seasonal effects when predicting the performance life of the overlay.

MOISTURE RELATED STRAINS

Environmental strains are produced not only by changes in temperature but also by changes in moisture content. The effects of moisture related strains are both seasonal and daily. Drying shrinkage continues to occur as the concrete ages. Drying shrinkage occurs more rapidly at the surface of the pavement where is easier for the water to escape into the atmosphere. Janssen (6) measured the moisture content at the top of the pavement to be as low as 50 percent saturated but the moisture content increases rapidly with depth, while the bottom of the pavement is near saturation. The bending stress created by this moisture gradient in a 203-mm slab was estimated to produce shrinkage cracks 19 mm deep assuming the tensile strength of the concrete was 2.8 MPa. Cracks this deep are not as significant in a 203-mm slab as they would be in a thin overlay. The strain gages in the test sections were used to determine the differential shrinkage that occurs between the top and bottom of the overlays and to characterize the effects of rain events on slab strains.

Daily Fluctuations in Moisture Content

First the effects of rain events on the response of the slab are presented. Figure 14 shows the time and magnitude of each rain event that occurred between July 9 and August 9. The two dates chosen for analysis were August 1 and August 8. August 1 was chosen because a rain event had not occurred for thirteen days prior to this date so the moisture content at the top of the overlay should be relatively low. August 8 followed 6 days of consecutive rain events so the

moisture content at the top of the overlay should have increased. Figure 15 and 16 show the relationship between strain and change in temperature on August 1 and 8 for both the top and bottom sensor of the 152-mm and 76-mm overlays. Both graphs show a rain event has little influence on the strains measured at the bottom of the slab. The difference in the strains measured at the top of the slab before and after the rain event was an increase of 50 microstrains for the 102-mm overlay and 75 microstrains for the 152-mm overlay for equivalent increases in temperature. The rate of expansion with change in temperature was constant before and after the rain event for both the top and bottom sensors. The increase in moisture content at the pavement surface caused the pavement to expand so the temperature at which the joints locked decreased by 5°C after the rain event even though the maximum strain remained constant. The bottom of the slab locked at the same temperature before and after the rain event indicating the moisture content at the bottom of the thin and ultra-thin overlays is not affected by a rain event.

The effect of the magnitude and duration of a rain event on the strain measured on the top portion of the 76-mm overlay was further evaluated. Comparisons were made between strain readings measured 7 days after a rain event (July 26), 13 days after a rain event (August 1), 1 day after a short but intense rain event (July 15), and 1 day after several days of low intensity rain events (August 8). Strain measured on the top sensor was plotted against change in temperature over a 24-hr period for all four days in figure 17. The lowest strains were measured on August 1, which was 13 days after a rain event. The strains measured on July 26 (7 days after a rain event) were the next lowest since the moisture content at the pavement surface was still less than that on days following a rain event. The strains were largest on August 8, showing that a slow rain lasting several days will increase the moisture content in the pavement surface more than one day with an intense rain event. It is interesting to note that the July 14 rain event had 13 mm more precipitation than the precipitation that accumulated between August 3 and August 8 and yet the strain was still higher on August 9 because the duration of the rain events was longer. This stresses the importance of considering the duration of the rain event and not just the rain intensity.

A summary of the temperatures at which the joints locked is provided below. The lower the moisture content at the surface of the slab the higher the temperature at which the joint will lock. This data indicates that the moisture content at the surface of the slab significantly influences the temperature required to lock the joint. This helps to explain why blow-ups typically occur on hot summer afternoons after it has rained.

Date	**Temperature the Joint Locked**
August 8	26°C
July 15	27°C
July 26	31°C
August 1	33°C

Long-Term Drying Shrinkage

The previous section looked at daily fluctuations associated with moisture-related strain. This section addresses long-term strains. Strains and temperatures were plotted in figure 18 for the first seven days after the 102-mm overlay was placed. The strain plotted represents both temperature and moisture related strain that develops over the first seven days. The initial strain was defined as the strain measured 45 minutes after the concrete was placed. The ambient temperatures were low so wet burlene and blankets were placed on the overlay for the first 4

days after paving. The blankets kept large temperature gradients from developing thereby significantly reducing construction-related curling. These curing techniques also helped to decrease early-age shrinkage. The shrinkage at the bottom and top of the overlay was measured by subtracting the initial strain measured 45 minutes after the paver passed from the strain measured at 1 month, 2 months, 1 year, 2 year, and 3 years from the time of construction. The thermal coefficient of the concrete was measured in the lab to be 9.5 x 10^{-6} per °C. This was used to correct the strains for changes in temperature so that the effects of drying shrinkage could be isolated. The results are shown in figure 19. Although the strain measured at the top of the overlay is relatively high compared to the bottom of the overlay, this is much less than the 1000 microstrains typically measured for 3 year old concrete containing gravel aggregate.(7) One reason the drying shrinkage in the overlay is lower than 1000 microstrains is re-wetting occurs in the overlay every time it rains. Wet curing also allowed the concrete to gain strength before drying shrinkage occurred so the concrete had sufficient strength to prevent cracking. The strength of the concrete for the overlay was also much higher than the tensile strength of the concrete in reference 7 (2.8 MPa vs. 4.3 MPa). The combination of the additional strength and the wet curing helped to prevent drying shrinkage cracking.

CONCLUSIONS

Large gradients develop in both TW and UTW but the short joint spacing and the bond between the asphalt and overlay limit the amount of curling that takes place. The bond strength did vary seasonally. Changes in bond strength greatly influence the stress from applied loads and the rate of strain with change in temperature so seasonal variations in bond strength must be accounted for when predicting the performance life. The rate of thermal strain is also dependent on the direction of the strain. Strains generated as the slab expands were larger than strains generated as the slab contracts for an equivalent change in temperature. Expansion of the slab is restrained as the joints locked up. The temperature the upper portion of the slab locked was significantly higher than the temperature the lower portion of the slab locked due to the increase in the amount of drying shrinkage that occurred on the top of the slab and the sawed joint provided additional room for expansion. The temperature at which the upper portion of the slab locked decreased after a rain event helping to explain why it is common for slab blow-ups to occur on hot afternoons after a rain event. Long-term moisture changes were also shown to influence strain magnitudes and joint lock-up temperatures.

Both thermal and moisture changes in the overlay have a significant effect on the shape of the slab. Strain measurements revealed the complexity of the relationship between changes in temperature and/or moisture and slab deformation. This relationship must be clearly defined before an analysis of the response of the overlay to an applied load can begin. This study helped characterize these relationships.

REFERENCES

1. Mack, J. W., Chung Lung Wu, S. Tarr and T. Refai, "Model Development and Interim Design Procedure Guidelines for Ultra-thin Whitetopping Pavements," Sixth International Purdue Conference on Concrete Pavement Design and Materials for High Performance, Vol.1, West Lafayette, IN, November 1997.

2. Packard, L. W., L. W. Cole, and J. E. Naughton, "Design of Ultra-thin Whitetopping for General Aviation Airport Pavements," 1999 Federal Aviation Administration Technology Transfer Conference, April 1999.

3. Wu, C. L., S. M. Refai, M. A. Nagi, and M. J. Sheehan, "Development of Ultra-thin Whitetopping Design Procedure," Portland Cement Association Research and Development Serial No. 2124, Skokie, IL, 1997.

4. Tarr, S. M., M. J. Sheehan and P. A. Okamoto, "Guidelines for the Thickness Design of Bonded Whitetopping Pavement in the State of Colorado – Final Report," Report No. CDOT-DTD-R-98-10, Colorado Department of Transportation Research Branch, Denver, CO, December 1998.

5. Bagate, M., B. F. McCullough and D. W. Fowler, "A Mechanistic Design for Thin-Bonded Concrete Overlay Pavements," Research Report 457-3, Center for Transportation Research, Austin, TX, September 1987.

6. Janssen, D. J., "Moisture in Portland Cement Concrete," Transportation Research Record 1121, Transportation Research Board, Washington, DC, 1987.

7. Mehta, P. K. and P. J. Monteiro, *Concrete: Structure, Properties, and Materials*, Second Edition, Prentice Hall, Englewood Cliffs, NJ, 1993.

ACKNOWLEGMENTS

The author would like to gratefully acknowledge the Federal Highway Administration and the Minnesota Local Road Research Board for their financial support in conducting this research. The author is also truly grateful to Mr. Aaron Fagerness for his continued dedication to this research effort and for helping generate the figures and table provided in this paper and to Dr. Mark Snyder for providing editorial comments. Finally, the author would like to thank Mr. Jack Herndon and the personnel at the Mn/ROAD Research Facility and her colleagues in the Minnesota Department of Transportation Research Office for their assistance during the construction of the test sections and with data collection.

DISCLAIMER

The contents of this report reflect the views of the author who is responsible for the facts and accuracy of the data presented herein. The contents do not necessarily reflect the views or policies of the Minnesota Department of Transportation. This report does not constitute a standard, specifications or regulations.

Table 1. Temperature differentials and gradients.

	MAXIMUMS											
	76-mm Overlay				102-mm Overlay				152-mm Overlay			
	Mid-Panel		Edge		Mid-Panel		Edge		Mid-Panel		Edge	
	Temp. Diff.	Gradient	Temp. Diff.	Gradient	Temp. Diff.	Gradient	Temp. Diff.	Gradient	Temp. Diff.	Gradient	Temp. Diff.	Gradient
Month	°C	°C/cm	°C	°C/cm	°C	°C/cm	°C	°C/cm	°C	°C/cm	°C	°C/cm
January	3.29	0.52	2.97	0.47	5.53	0.56	5.71	0.64	6.13	0.44	4.60	0.33
February	3.62	0.57	3.88	0.61	4.25	0.43	4.28	0.48	6.93	0.50	6.68	0.48
March	6.00	0.95	4.64	0.73	6.88	0.70	5.63	0.63	11.58	0.83	9.30	0.67
April	6.32	1.00	5.13	0.81	7.92	0.81	6.92	0.77	12.37	0.89	10.02	0.72
May	6.66	1.05	5.48	0.86	7.94	0.81	6.88	0.77	12.03	0.86	9.61	0.69
June	6.42	1.01	5.55	0.88	7.64	0.78	7.03	0.79	11.95	0.86	9.43	0.68
July	7.78	1.23	7.02	1.11	7.50	0.76	6.64	0.74	13.33	0.96	10.31	0.74
August	6.81	1.07	6.27	0.99	7.04	0.72	6.67	0.75	13.12	0.94	10.40	0.74
September	5.55	0.88	5.23	0.83	6.89	0.70	5.72	0.64	10.23	0.73	8.63	0.62
October	4.58	0.72	3.27	0.52	5.12	0.52	3.28	0.37	8.00	0.57	6.13	0.44
November	3.78	0.60	2.80	0.44	4.14	0.42	2.98	0.33	6.90	0.49	6.20	0.44
December	3.18	0.50	2.80	0.44	2.95	0.30	2.42	0.27	6.63	0.47	5.83	0.42

	MINIMUMS											
	76-mm Overlay				102-mm Overlay				152-mm Overlay			
	Mid-Panel		Edge		Mid-Panel		Edge		Mid-Panel		Edge	
	Temp Diff	Gradient	Temp Diff	Gradient	Temp Diff	Gradient	Temp Diff	Gradient	Temp Diff	Gradient	Temp Diff	Gradient
Month	°C	°C/cm	°C	°C/cm	°C	°C/cm	°C	°C/cm	°C	°C/cm	°C	°C/cm
January	-2.93	-0.46	-2.83	-0.45	-2.14	-0.22	-1.83	-0.21	-5.71	-0.41	-5.44	-0.39
February	-3.08	-0.49	-3.17	-0.50	-3.02	-0.31	-2.78	-0.31	-5.38	-0.39	-4.96	-0.36
March	-3.43	-0.54	-3.36	-0.53	-3.32	-0.34	-2.84	-0.32	-4.82	-0.35	-4.03	-0.29
April	-2.42	-0.38	-2.59	-0.41	-3.38	-0.34	-2.77	-0.31	-4.10	-0.29	-4.02	-0.29
May	-2.36	-0.37	-2.52	-0.40	-3.31	-0.34	-2.62	-0.29	-3.68	-0.26	-3.85	-0.28
June	-4.64	-0.73	-4.72	-0.74	-4.42	-0.45	-2.95	-0.33	-3.91	-0.28	-4.68	-0.34
July	-5.17	-0.82	-5.36	-0.84	-6.07	-0.62	-4.91	-0.55	-5.07	-0.36	-6.11	-0.44
August	-2.90	-0.46	-2.82	-0.44	-3.56	-0.36	-3.33	-0.37	-3.72	-0.27	-4.60	-0.33
September	-2.67	-0.42	-2.91	-0.46	-4.16	-0.42	-4.16	-0.47	-4.70	-0.34	-4.47	-0.32
October	-2.52	-0.40	-2.86	-0.45	-4.17	-0.42	-4.11	-0.46	-5.31	-0.38	-4.58	-0.33
November	-2.62	-0.41	-2.80	-0.44	-3.87	-0.39	-3.74	-0.42	-5.37	-0.38	-5.28	-0.38
December	-4.13	-0.65	-3.48	-0.55	-3.50	-0.36	-3.60	-0.40	-8.82	-0.63	-8.46	-0.61

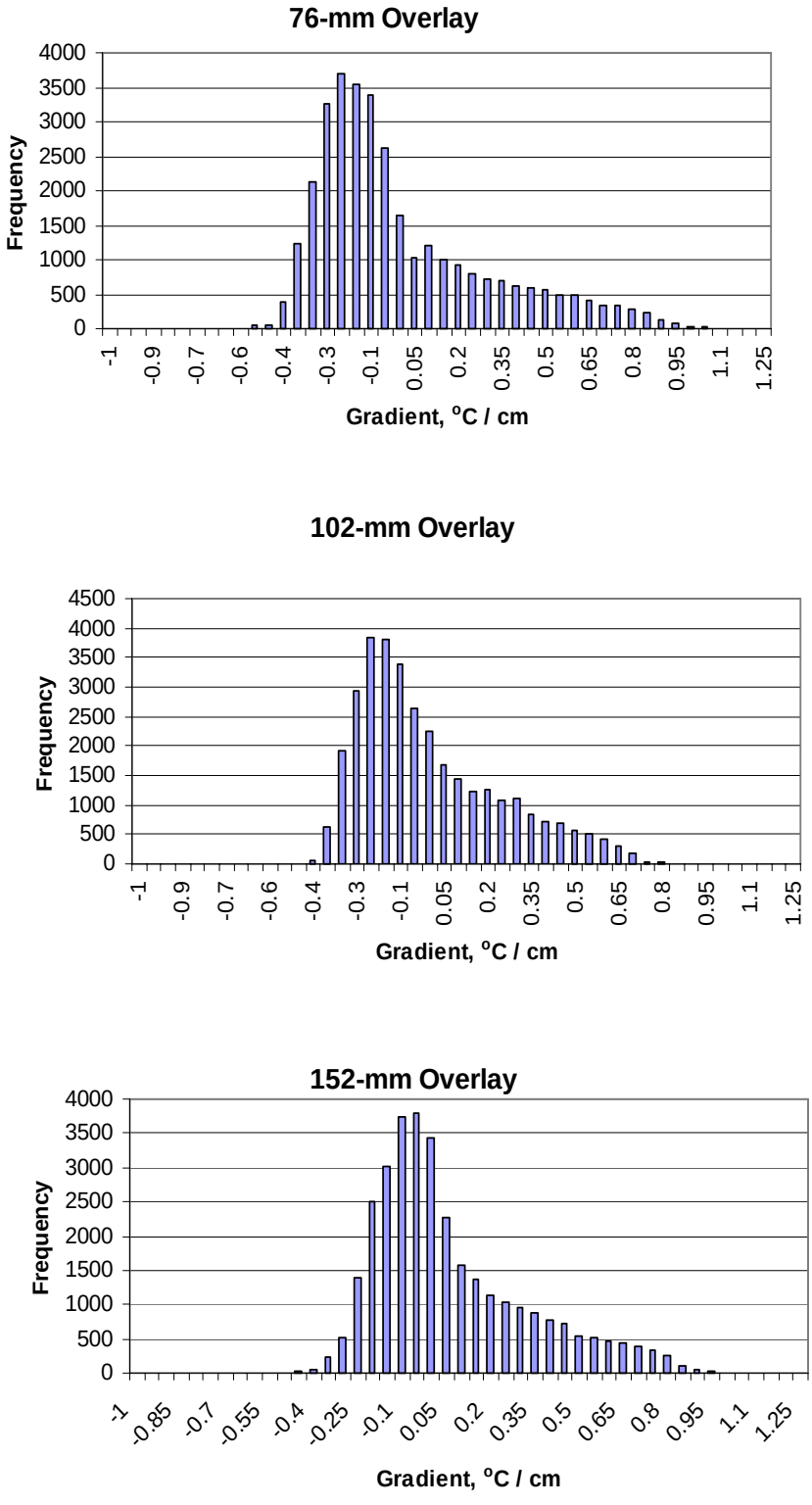

Figure 1. Frequency distributions of linear temperature gradients measured at midpanel.

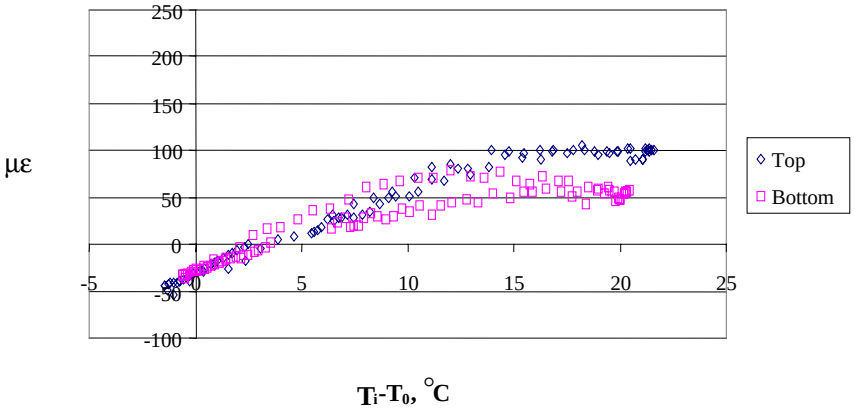

Figure 2. 76-mm Overlay - Gages at Midpanel. – May.

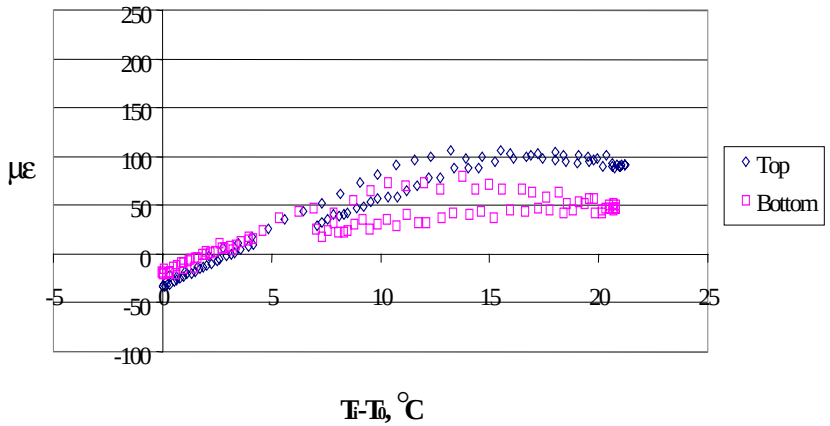

Figure 3. 76-mm Overlay – Gages Adjacent to Longitudinal Jt.– May.

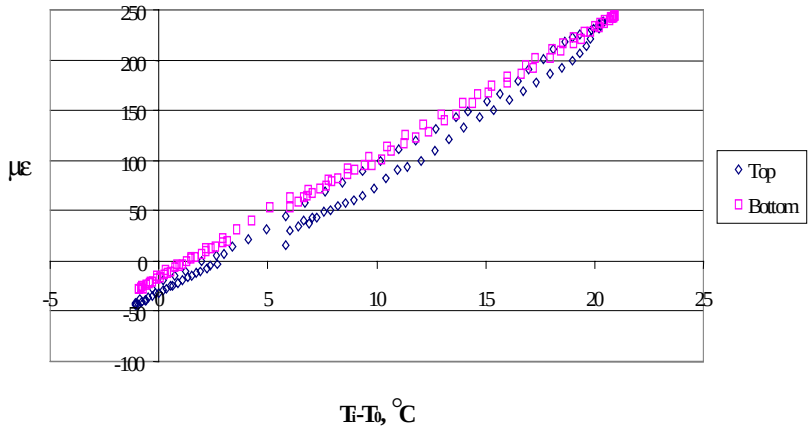

Figure 4. 76-mm Overlay – Gages Adjacent to Transverse Joint - May.

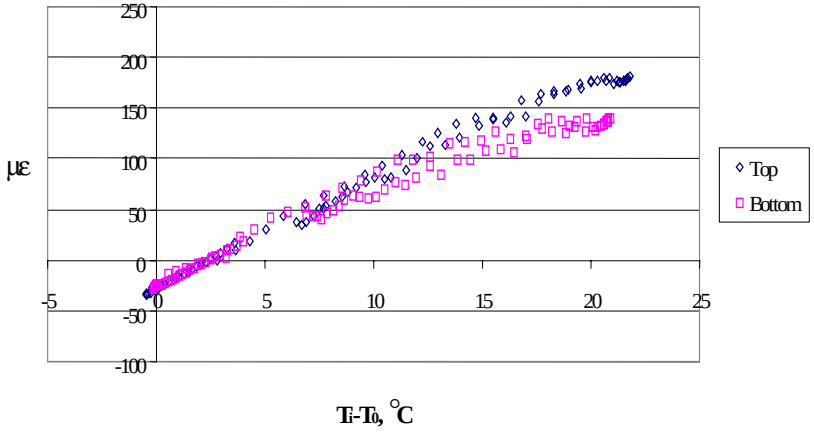

Figure 5. 76-mm Overlay – Gages at Corner Diagonal - May.

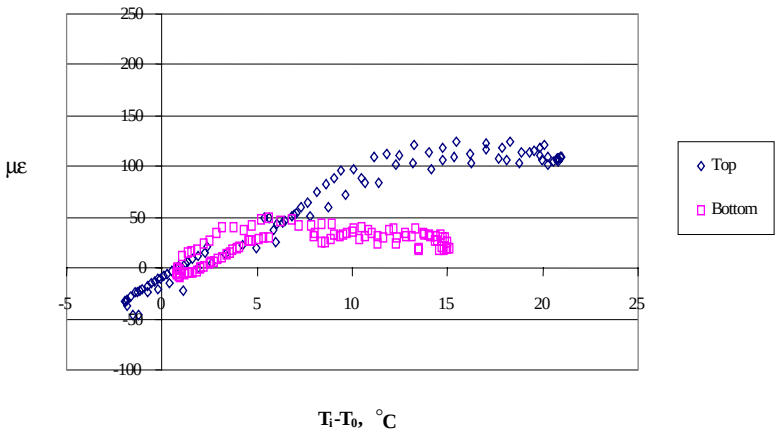

Figure 6. 152-mm Overlay – Gages at Midpanel - May.

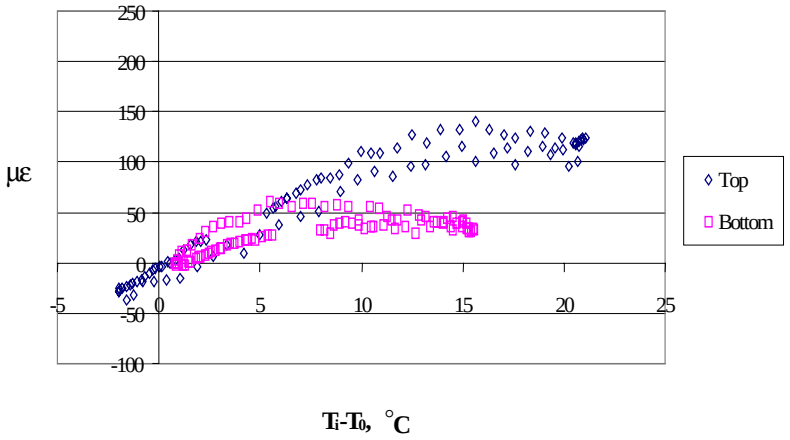

Figure 7. 152-mm Overlay – Gages at Midpanel – May.

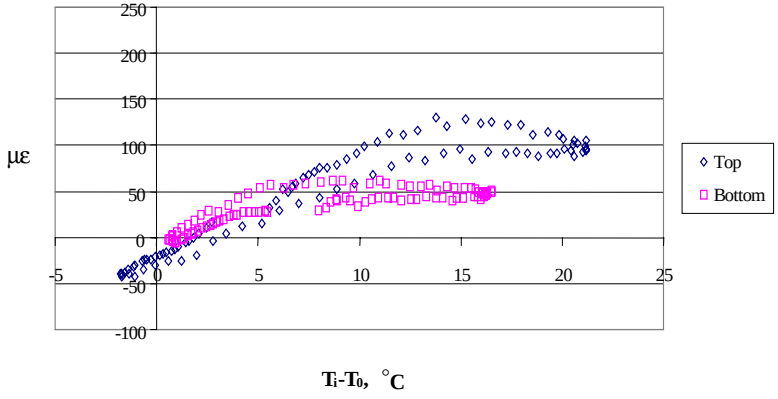

Figure 8. 152-mm Overlay – Gages Adjacent to Longitudinal Joint - May.

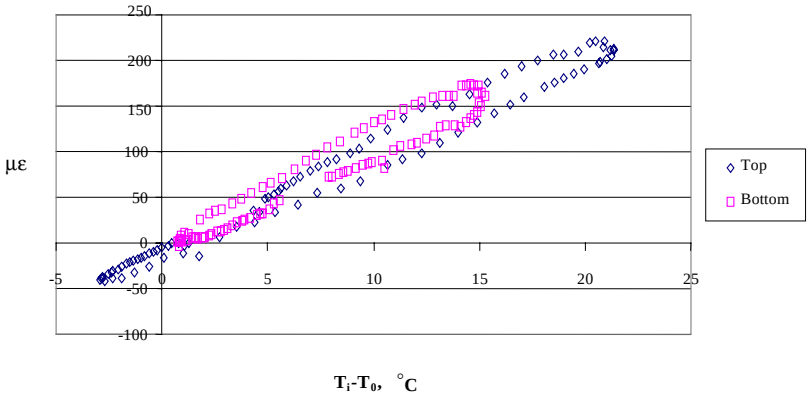

Figure 9. 152-mm Overlay –Gages Adjacent to Transverse Joint - May.

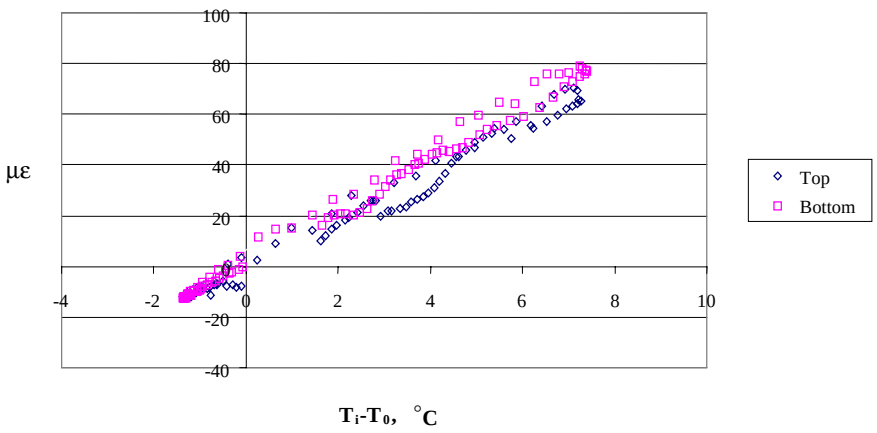

Figure 10. 76-mm Overlay – Gages Adjacent to Transverse Joint - December. (Note: This scale is different from previous graphs.)

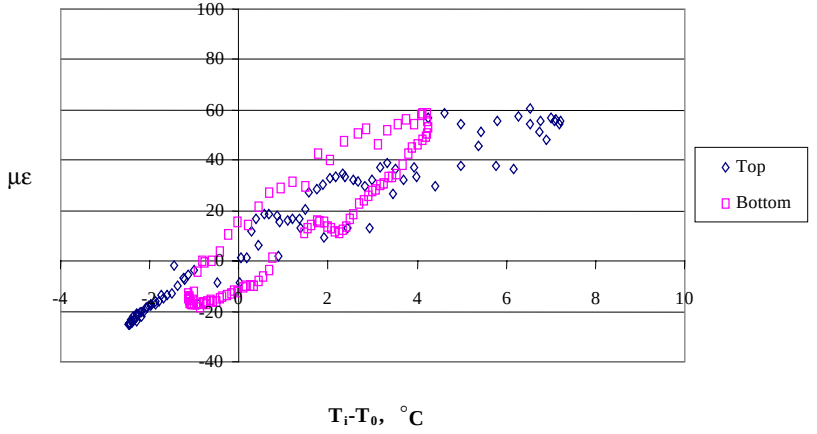

Figure 11. 152-mm Overlay – Gages Adjacent to Transverse Jt. - December. (Note: This scale is different from previous graphs.)

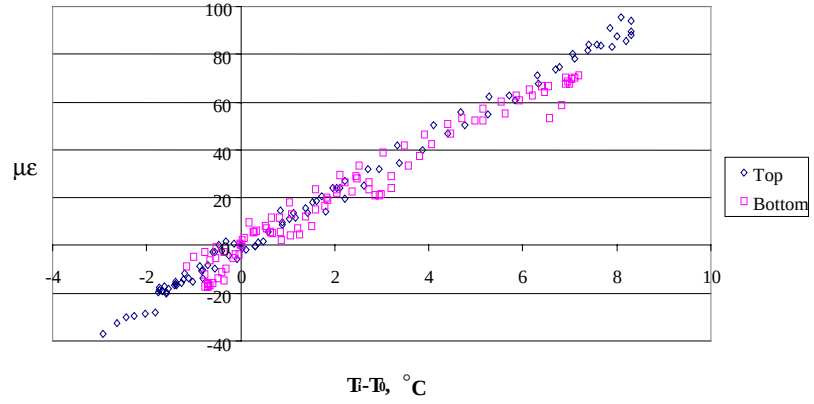

Figure 12. 102-mm Overlay – Gages Adjacent to Transverse Joint - October. (Note: This scale is different from previous graphs.)

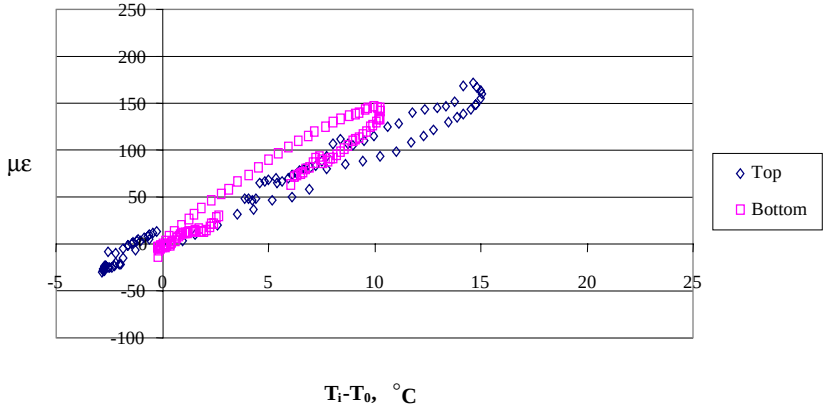

Figure 13. 152-mm Overlay – Gages Adjacent to Transverse - Joint - October.

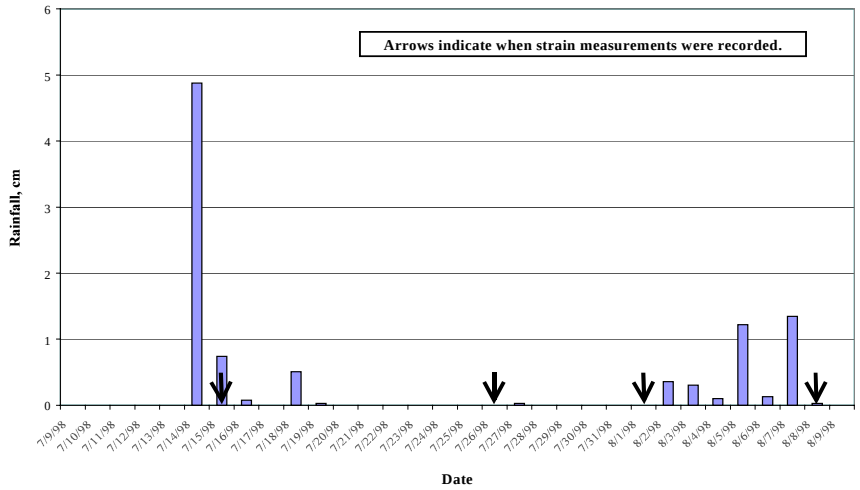

Figure 14. Precipitation data for July 9 through August 9.

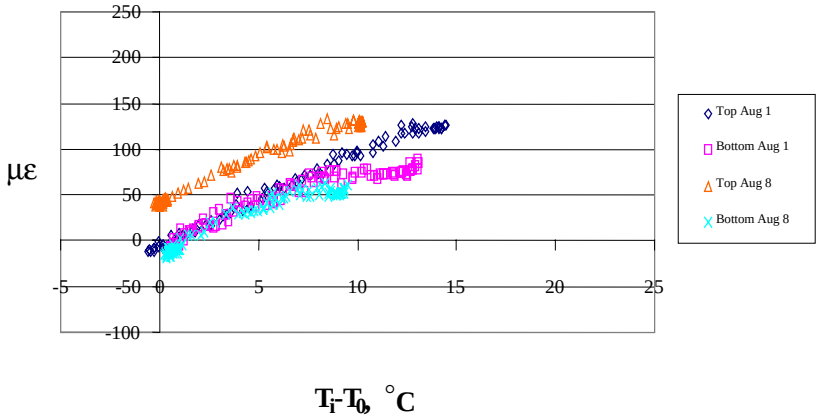

Figure 15. 102-mm Overlay – Gages at Midpanel - July/August.

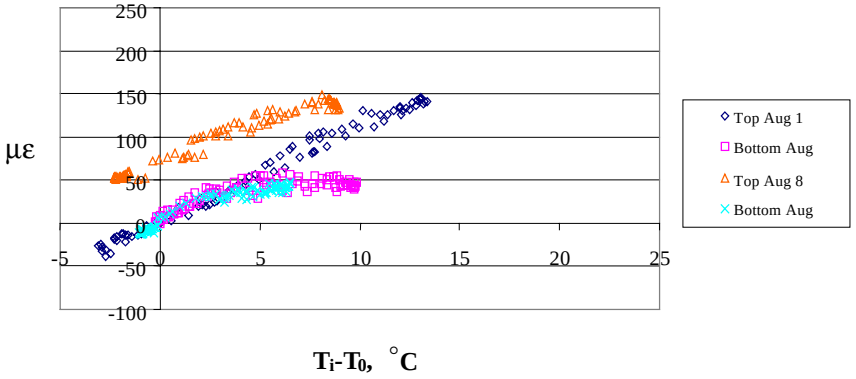

Figure 16. 152-mm Overlay – Gages at Midpanel - July/August.

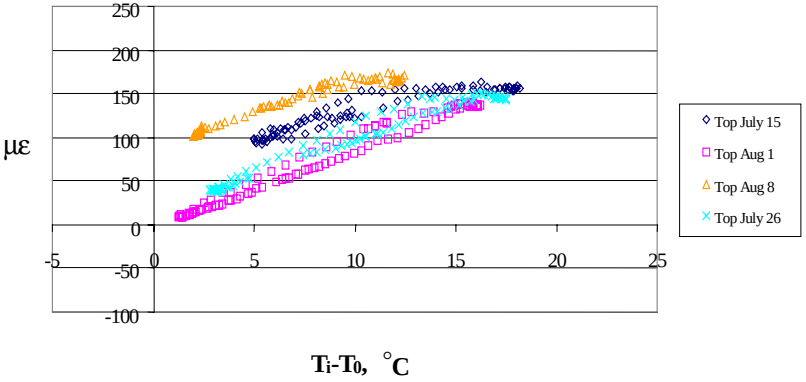

Figure 17. 76-mm Overlay – Gages Adjacent to Longitudinal Joint - July/August.

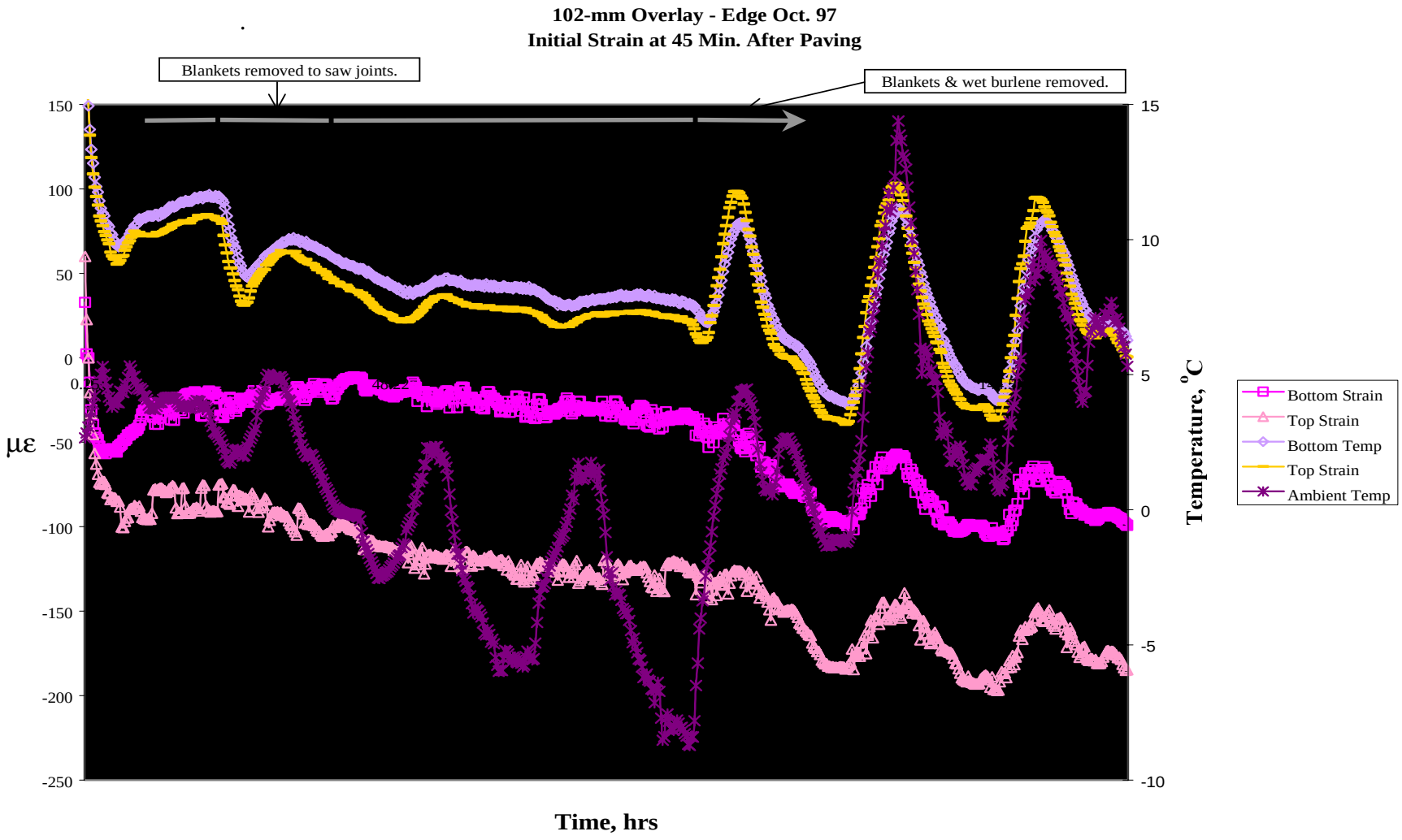

Figure 18. Temperature and strain data for first 7 days after construction.

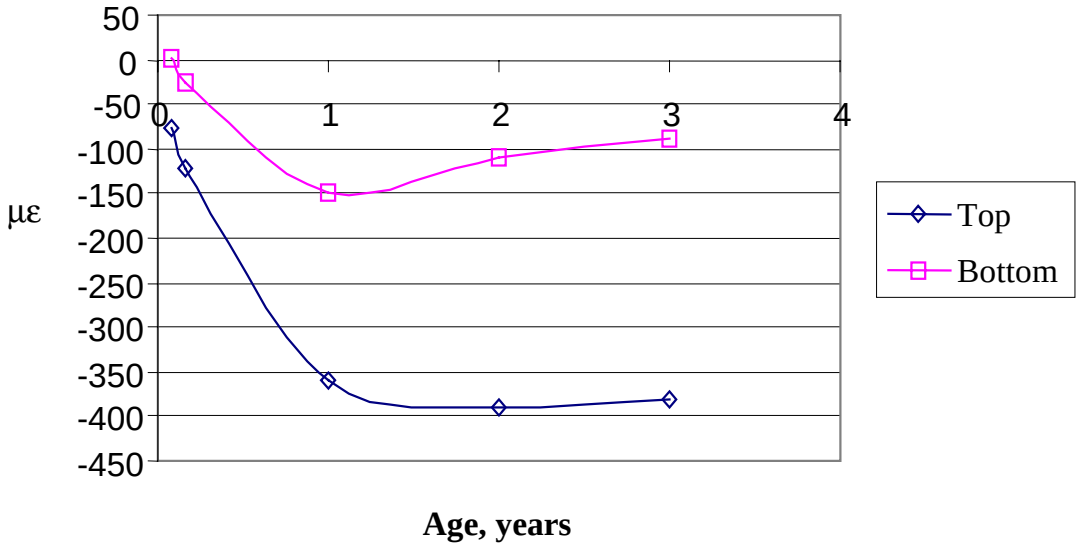

Figure 19. Drying shrinkage measured for 102-mm Overlay.